GAIMS – Generalized Ab Initio Multiple Spawning for both Internal Conversion and Intersystem Crossing Processes

Basile F. E. Curchod,[1,2] Clemens Rauer,[3] Philipp Marquetand,[3] Leticia González,[3] and Todd J. Martínez[1,2,a)]

[1]*Department of Chemistry and the PULSE Institute, Stanford University, Stanford, CA 94305, USA*

[2]*SLAC National Accelerator Laboratory, Menlo Park, CA 94025, USA*

[3]*Institute of Theoretical Chemistry, University of Vienna Währinger Straße 17, 1090 Vienna, Austria*

[a)] E-mail: toddjmartinez@gmail.com

Full Multiple Spawning is a formally exact method to describe the excited-state dynamics of molecular systems beyond the Born-Oppenheimer approximation. However, it has been limited until now to the description of radiationless transitions taking place between electronic states with the same spin multiplicity. This Communication presents a generalization of the Full and Ab Initio Multiple Spawning methods to both internal conversion (mediated by nonadiabatic coupling terms) and intersystem crossing events (triggered by spin-orbit coupling matrix elements) based on a spin-diabatic representation. The results of two numerical applications, a model system and the deactivation of thioformaldehyde, validate the presented formalism and its implementation.

I. Introduction

Nonadiabatic molecular dynamics – coupled electron-nuclear dynamics beyond the Born-Oppenheimer approximation – is a key technique for investigating photochemical and photophysical processes of molecules. However, most of the nonadiabatic methods commonly employed focus only on internal conversion (IC), i.e., electronic state transitions that conserve spin multiplicity. They often neglect *intersystem crossing* (ISC) events which couple electronic states with differing spin multiplicity, due to relativistic spin-orbit coupling (SOC).[1] Far from being a curiosity, ISC plays an important role in the deactivation process of organic molecules[2-4] and metal complexes[5] that are used in energy-related devices.[6-7]

Apart from grid-based exact quantum dynamics for low dimensional problems,[8] few nonadiabatic dynamics methods have been extended to include SOC effects and, therefore, to describe ISC.[9] As one example, the Multiconfiguration Time-Dependent Hartree (MCTDH) technique has been used to understand the role of intersystem crossing in benzene photophysics.[10] Trajectory surface hopping (TSH), which approximates the dynamics of a nuclear wavepacket by a swarm of independent classical trajectories, has also been modified to incorporate SOC effects.[11-15] Freedom in the choice of different spin representations[11-14, 16] or hopping schemes[17] has resulted in a plethora of TSH algorithms, which are, however, prone to shortcomings of the independent trajectory approximation.[18-19] In particular, the spin-diabatic representation for including SOC in TSH has been questioned due to a lack of rotational invariance for electronic population dynamics.[13] It can further lead to problematic results whenever sublevels are grouped in single multiplet states.[13, 16]

An ideal method for describing both IC and ISC processes would be (*i*) derivable from *first principles*, (*ii*) able to treat medium to large molecular systems, (*iii*) compatible with on-the-fly calculations of electronic quantities, and (*iv*) able to adequately describe coherence and decoherence effects during nonadiabatic events. Full Multiple Spawning (FMS),[20-21] or its ab initio version AIMS,[22-23] fulfills all of the previously listed requirements, combing the computational efficiency of a trajectory-based methods with quantum dynamics that is *in principle* exact (in the limit of a large enough basis set).

In short, FMS represents a nuclear wavefunction by a swarm of coupled frozen Gaussian functions following classical trajectories.[22-24] The number of trajectory basis functions used to describe the nuclear wavepacket is adapted during the dynamics – through so-called "spawning" events – to accurately describe wavepacket bifurcation in nonadiabatic regions. In the limit of a complete basis set and exact

evaluation of all the requisite matrix elements, FMS constitutes a formally exact solution of the time-dependent Schrödinger equation. In the following, we show how FMS and AIMS can be extended to the description of both IC and ISC processes and present the resulting Generalized FMS and AIMS (GFMS and GAIMS) methods and their implementation.

II. Theory

The original derivation of the FMS method begins with the standard molecular Hamiltonian,[22] defined as the sum of the nuclear kinetic energy operator and the electronic Hamiltonian,

$$\hat{H}_{mol}(\mathbf{r},\mathbf{R}) = \hat{T}_N + \hat{H}_{el}(\mathbf{r},\mathbf{R}) = \hat{T}_N + \hat{T}_e + \hat{V}_{ee}(\mathbf{r}) + \hat{V}_{eN}(\mathbf{r},\mathbf{R}) + \hat{V}_{NN}(\mathbf{R}) \tag{1}$$

where $\hat{T}_e$ is the electronic kinetic energy operator and $\hat{V}_{ee}(\mathbf{r})$, $\hat{V}_{eN}(\mathbf{r},\mathbf{R})$, and $\hat{V}_{NN}(\mathbf{R})$ are the electron-electron, electron-nucleus, and nucleus-nucleus potential energy operators, respectively. The collective variables for electronic and nuclear positions are denoted by $\mathbf{r}$ and $\mathbf{R}$, respectively. The Hamiltonian in Eq.(1) is non-relativistic and therefore neglects all terms related to both nuclear and electronic spin.

Including SOC effects in the framework of the time-dependent Schrödinger equation necessitates the derivation and approximation of new extended electronic Hamiltonians from the Dirac-Coulomb-Breit equation.[25] The Breit-Pauli Hamiltonian is commonly employed and its most important parts[26] comprise the non-relativistic Hamiltonian of Eq.(1), a scalar relativistic part containing the mass-velocity and Darwin terms, and a spin-orbit coupling Hamiltonian.[25, 27] We note that scalar relativistic effects, when important, are often accounted for in quantum chemistry by using effective core potentials.[28] Incorporating the SOC Hamiltonian in the electronic Hamiltonian,[27, 29-31] we obtain a molecular Hamiltonian accounting for the electronic spin s,

$$\hat{H}(\mathbf{x},\mathbf{R}) = \hat{T}_N + \hat{H}_{el}(\mathbf{r},\mathbf{R}) + \hat{H}_{SOC}(\mathbf{x},\mathbf{R}) \tag{2}$$

with $\mathbf{x} = (\mathbf{r}, s)$. Inserting Eq.(2) into the time-dependent Schrödinger equation leads to the starting equation for our extension of FMS including SOC:

$$i\frac{\partial \Psi(\mathbf{x},\mathbf{R},t)}{\partial t} = \hat{H}(\mathbf{x},\mathbf{R})\Psi(\mathbf{x},\mathbf{R},t) \tag{3}$$

The following derivation will use electronic states obtained from a spin-free electronic Hamiltonian as a basis, i.e., each electronic state is an eigenstate of both the total spin operator $\hat{S}^2$ and the spin projection operator $\hat{S}_z$.[13] The time-dependent molecular wavefunction is represented by a Born-Huang expansion[32] in the aforementioned spin-diabatic electronic basis,

$$\Psi(\mathbf{x},\mathbf{R},t)=\sum_{J}\sum_{M_{S_J}=-S_J}^{S_J}\Omega_J^{M_{S_J}}(\mathbf{R},t)\Phi_J^{M_{S_J}}(\mathbf{x};\mathbf{R}) \tag{4}$$

where $\Phi_J^{M_{S_J}}(\mathbf{x};\mathbf{R})=\left|J,M_{S_J}\right\rangle$ is the electronic wavefunction for the *J*th state with spin multiplicity $(2S_J+1)$ and spin-projection eigenvalue M_{S_J}. While the formalism is completely general, we focus our attention on singlet (*S*=0) and triplet (*S*=1) electronic states, the latter having M_S values of -1, 0, or +1. The FMS ansatz[20-21] for the nuclear wavefunction becomes

$$\Omega_J^{M_{S_J}}(\mathbf{R},t)=\sum_{k'=1}^{N_{J,M_{S_J}}(t)}C_{k'}^{J,M_{S_J}}(t)\chi_{k'}^{J,M_{S_J}}(\mathbf{R};\overline{\mathbf{R}}_{k'}^{J,M_{S_J}}(t),\overline{\mathbf{P}}_{k'}^{J,M_{S_J}}(t),\overline{\gamma}_{k'}^{J,M_{S_J}}(t),\boldsymbol{\alpha}_{k'}^{J,M_{S_J}}) \tag{5}$$

which expresses the nuclear wavefunction for the electronic state $\left|J,M_{S_J}\right\rangle$ as a linear combination of multidimensional frozen Gaussians $\chi_{k'}^{J,M_{S_J}}$ and corresponding complex coefficients $C_{k'}^{J,M_{S_J}}(t)$. Each term of the linear combination is called a trajectory basis function (TBF). The time-dependent position $\overline{\mathbf{R}}_{k'}^{J,M_{S_J}}(t)$ and momentum $\overline{\mathbf{P}}_{k'}^{J,M_{S_J}}(t)$ centers for each frozen Gaussian are propagated using classical Hamilton's equations, while the nuclear phase $\overline{\gamma}_{k'}^{J,M_{S_J}}(t)$ is time-evolved semiclassically.[22] We note here that the time-dependent parameters in the Gaussian functions could be time-evolved in different ways, leading to techniques for nonadiabatic dynamics like the direct dynamics variational multi-configurational Gaussian[33] (DD-vMCG) or the multiconfiguration-Ehrenfest approach[34] (MCE), for example.

Inserting Eqs. (5) and (4) in Eq.(3) leads to a set of equations of motion for the complex amplitudes in Eq.(5). After left-projection by $\left\langle\chi_k^{I,M_{S_I}}\Phi_I^{M_{S_I}}\right|$, we obtain

$$\frac{d\mathbf{C}^{I,M_{S_I}}(t)}{dt}=-i\left(\mathbf{S}^{-1}\right)^{II,M_{S_I}M_{S_I}}\left\{\left[\mathbf{H}^{II,M_{S_I}M_{S_I}}-i\dot{\mathbf{S}}^{II,M_{S_I}M_{S_I}}\right]\mathbf{C}^{I,M_{S_I}}(t)+\sum_{J}\sum_{M_{S_J}=-S_J}^{S_J}\mathbf{H}^{IJ,M_{S_I}M_{S_J}}\mathbf{C}^{J,M_{S_J}}(t)\right\} \tag{6}$$

where bold symbols indicate vectors or matrices in the basis of Gaussian functions. The overlap matrices are defined by $S_{k,k'}^{IJ,M_{S_I}M_{S_J}}=\left\langle\chi_k^{I,M_{S_I}}\middle|\chi_{k'}^{J,M_{S_J}}\right\rangle_{\mathbf{R}}\delta_{IJ}\delta_{M_{S_I}M_{S_J}}$ and $\dot{S}_{k,k'}^{IJ,M_{S_I}M_{S_J}}=\left\langle\chi_k^{I,M_{S_I}}\middle|\frac{\partial}{\partial t}\middle|\chi_{k'}^{J,M_{S_J}}\right\rangle_{\mathbf{R}}\delta_{IJ}\delta_{M_{S_I}M_{S_J}}$. A general Hamiltonian matrix element in Eq. (6) has the form

$$H_{kk'}^{IJ,M_{S_I}M_{S_J}} = \left\langle \chi_k^{I,M_{S_I}} \middle| \hat{T}_{nuc} \middle| \chi_{k'}^{J,M_{S_J}} \right\rangle_{\mathbf{R}} \delta_{IJ}\delta_{M_{S_I}M_{S_J}} + \left\langle \chi_k^{I,M_{S_I}} \middle| E_I^{el} \middle| \chi_{k'}^{J,M_{S_J}} \right\rangle_{\mathbf{R}} \delta_{IJ}\delta_{M_{S_I}M_{S_J}}$$
$$- \sum_{\rho=1}^{3N} \left\langle \chi_k^{I,M_{S_I}} \middle| \left(\mathbf{d}_{IJ}^{M_{S_I}M_{S_J}}\right)_\rho \frac{1}{m_\rho}\frac{\partial}{\partial R_\rho} \middle| \chi_{k'}^{J,M_{S_J}} \right\rangle_{\mathbf{R}} \delta_{M_{S_I}M_{S_J}} - \sum_{\rho=1}^{3N} \frac{1}{2m_\rho} \left\langle \chi_k^{I,M_{S_I}} \middle| \left(D_{IJ}^{M_{S_I}M_{S_J}}\right)_\rho \middle| \chi_{k'}^{J,M_{S_J}} \right\rangle_{\mathbf{R}} \delta_{M_{S_I}M_{S_J}} \quad (7)$$
$$+ \left\langle \chi_k^{I,M_{S_I}} \middle| \left\langle \Phi_I^{M_{S_I}} \middle| \hat{H}_{SOC} \middle| \Phi_J^{M_{S_J}} \right\rangle_{\mathbf{x}} \middle| \chi_{k'}^{J,M_{S_J}} \right\rangle_{\mathbf{R}} .$$

The first two terms couple TBFs evolving on the same electronic state with the same sublevel (Fig. 1a, dotted arrows). The third and fourth terms in Eq.(7) couple TBFs evolving on different electronic states but having the same S and M_S values (Fig. 1a, dashed arrows). These terms depend on the first-order nonadiabatic coupling vectors $\mathbf{d}_{IJ}^{M_{S_I}M_{S_J}}$ and second-order nonadiabatic coupling $D_{IJ}^{M_{S_I}M_{S_J}}$, where the latter is usually neglected in nonadiabatic molecular dynamics.[22] The novelty of GFMS resides in the last term of Eq.(7) which allows for amplitude transfer between electronic states with different spin multiplicity, according to the rules of SOC (Fig. 1a, continuous arrows), and fully preserves rotational invariance. In addition, this last term can also couple TBFs evolving on states that have the same spin multiplicity S, but only if the conditions $S_I = S_J > 0$ and $\Delta M_S = 0, \pm 1$ are fulfilled. It is important to note that any definition[1] of the operator $\hat{H}_{SOC}$ can be used in Eq.(7).

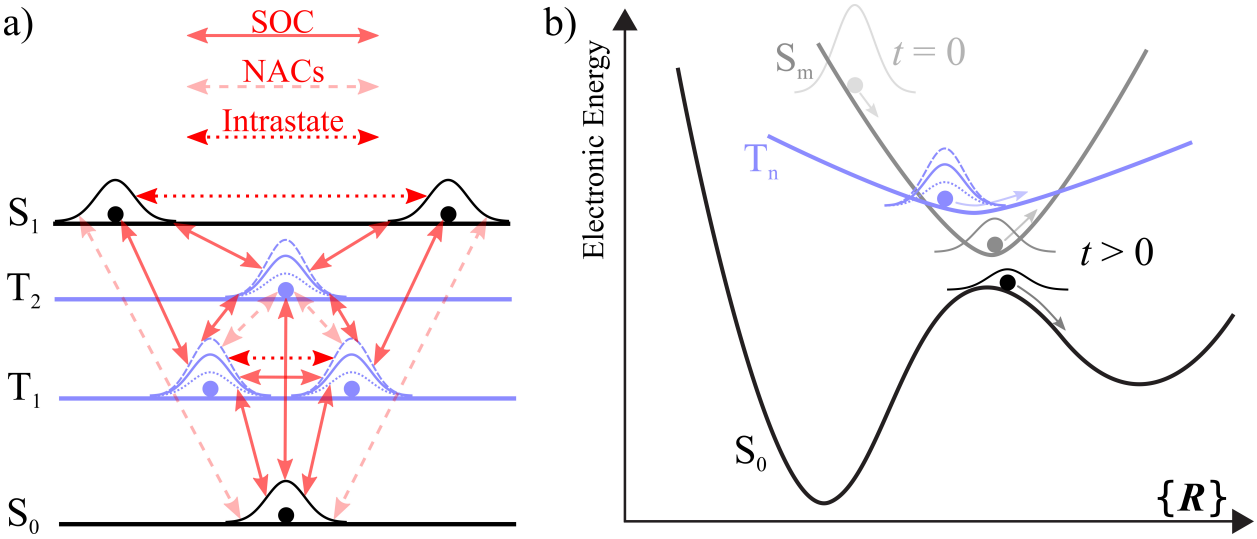

Figure 1. a) General representation of the coupling pattern between TBFs in GFMS for a case with two singlet and two triplet states. The Gaussian shape symbolizes the different TBFs (black=singlet, blue=triplet), where a continuous line is used for M_S=0 states, while dashed and dotted lines represent M_S=-1 and M_S=1 for triplet states. These TBFs evolve along a classical trajectory represented by the filled circle. Intrastate (dotted arrow) and nonadiabatic (dashed arrows) couplings are present between TBFs evolving in electronic states with the same spin multiplicity (as in the standard FMS method), while GFMS introduces an important number of additional couplings due to SOC (plain arrows). Note that a more detailed representation of the couplings requires the use of separate arrows for each possible coupling between sublevels (not shown). b) Schematic representation of the GFMS method. A TBF is initiated in S_m at time t=0 (gray) and will at later time spawn TBFs both in T_n (blue) and in S_0 (black).

A key feature of the FMS method is that it uses an adaptive basis set to ensure an accurate description of nonadiabatic processes. The number of TBFs describing the nuclear wavefunction in state $\left|I,M_{S_I}\right\rangle$, $N_{I,M_{S_I}}(t)$, will indeed change in time as a result of spawning events. In short, a TBF entering a region of strong nonadiabaticity – detected using an effective coupling – can under certain conditions spawn a new TBF on the coupled electronic state (Fig. 1b). Upon spawning, the size of the matrices in Eq. (6) is extended and the resulting coupled propagation of the expanded set of TBFs allows for an exchange of nuclear amplitude between electronic states. For detailed discussions about the spawning algorithm between same-spin states, the reader is referred to previous work.[22, 24, 35] In GFMS, the spawning algorithm needs to be extended to allow for spawning between spin-orbit coupled states. Based on an already proposed effective coupling between diabatic states,[22] we suggest to measure the effective SOC strength between state *I* and state *J* at the position of TBF *k* as:

$$\Lambda_{IJ}^{eff}\left(\mathbf{R}_k\right)=\frac{\left(\sum_{M_{S_I}=-S_I}^{S_I}\sum_{M_{S_J}=-S_J}^{S_J}\left|\left\langle\Phi_I^{M_{S_I}}\left(\mathbf{R}_k\right)\middle|\hat{H}_{SOC}\middle|\Phi_J^{M_{S_J}}\left(\mathbf{R}_k\right)\right\rangle_{\mathbf{x}}\right|^2\right)^{1/2}}{\left|E_J^{el}\left(\mathbf{R}_k\right)-E_I^{el}\left(\mathbf{R}_k\right)\right|}. \tag{8}$$

This rotationally-invariant spawning measure indicates the overall coupling between the sublevels of state *I* and those of state *J*. If $\Lambda_{IJ}^{eff}\left(\mathbf{R}_k\right)$ is higher than a certain threshold value, the spawning mode is triggered and a new TBF will be created in each sublevel of the electronic state *J* (see Fig. 1b).[36]

Ab Initio Multiple Spawning[22-24] uses FMS nuclear dynamics combined with ab initio electronic structure calculations, allowing for an on-the-fly solution of the molecular time-dependent Schrödinger equation. Two approximations simplify the application of FMS to molecules, namely the saddle point and the independent first generation (IFG) approximations. The (zeroth-order) saddle-point approximation is used to compute the integrals over nuclear degrees of freedom that appear in the Hamiltonian matrix.[22] Extending the saddle-point approximation to the calculation of SOC matrix elements in Eq.(7) is straightforward:

$$\left\langle\chi_k^{I,M_{S_I}}\middle|\left\langle\Phi_I^{M_{S_I}}\middle|\hat{H}_{SOC}\middle|\Phi_J^{M_{S_J}}\right\rangle_{\mathbf{x}}\middle|\chi_{k'}^{J,M_{S_J}}\right\rangle_{\mathbf{R}}=\left\langle\chi_k^{I,M_{S_I}}\middle|H_{SOC,IJ}^{M_{S_I}M_{S_J}}\middle|\chi_{k'}^{J,M_{S_J}}\right\rangle_{\mathbf{R}}\approx H_{SOC,IJ}^{M_{S_I}M_{S_J}}\left(\mathbf{R}_{kk'}^{(c)}\right)\left\langle\chi_k^{I,M_{S_I}}\middle|\chi_{k'}^{J,M_{S_J}}\right\rangle_{\mathbf{R}} \tag{9}$$

where $\mathbf{R}_{kk'}^{(c)}$ is the centroid position between TBFs *k* and *k*'. It is important to realize that the quality of the saddle-point approximation is expected to be especially good for SOC matrix elements, as they are

usually slowly varying with respect to the nuclear position. The IFG approximation proposes that the initial TBFs, whose initial positions and momenta are usually sampled from a Wigner distribution, are run independently, i.e. the interactions between initial TBFs are neglected. Each initial TBF however remains fully coupled with any child TBFs it will generate in the course of the nonadiabatic dynamics. For more information on these approximations, the interested reader is referred to different reviews on AIMS.[9, 22, 37-38]

To summarize, GFMS is a generalization to the *in principle* exact method FMS for the description of both IC and ISC processes. The GAIMS technique, which is amenable to molecules, is obtained by applying the IFG and saddle-point approximations to GFMS.

III. Test applications

The proposed AIMS extension to SOC is first tested on a model system recently proposed by Persico and coworkers.[13] The model comprises a singlet (S_1) and a triplet state (T_1), which cross at x=10 bohr and both have a dissociative character (continuous curves in Fig. 2a-c). All SOC matrix elements between the singlet and the triplet sublevels change sign at a given position, x_s, that can therefore be used as a parameter to tune the strength of intersystem crossing processes. For example, x_s=10 bohr leads to weak coupling between the electronic states, as the SOC is small around the point of crossing between the singlet and the triplet state (Fig. 2a). In contrast, when the sign change of the SOC takes place away from the states crossing point, e.g. x_s=8 bohr, the intersystem crossing is strong as $\left|H^{00}_{SOC,S_1T_1}\right|$ and $\left|H^{01}_{SOC,S_1T_1}\right| = \left|H^{0-1}_{SOC,S_1T_1}\right|$ are equal to 219.5 and 155.2 cm^{-1}, respectively, at the point of crossing (Fig. 2c). Therefore, varying x_s allows testing GAIMS for different SOC strength conditions.

The GAIMS dynamics is based on 200 initial conditions, sampled from the Wigner distribution of the initial Gaussian wavefunction, as defined in Ref. [13] (its corresponding probability density is represented in Fig. 2a). As mentioned in the previous section, GAIMS uses both the IFG and the saddle-point approximation, meaning that perfect agreement with an exact solution is not expected. It is however only within these two approximations that GAIMS can be routinely applied to molecular systems, and the goal in the following is to validate the general accuracy of GAIMS with respect to exact calculations. GAIMS reproduces the exact results, obtained by solving the TDSE,[13] both qualitatively and quantitatively, within a maximum deviation of 7%, for three different cases of SOC coupling strength (right panel of Fig. 2). Furthermore, Fig. 2 shows the results for uncorrected spin-diabatic TSH dynamics,[13] with the three sublevels of the triplet state grouped into a single TSH

amplitude. In this approximated formalism, TSH does not capture sign changes for the SOC and is unable to qualitatively describe ISC events, whenever the sign change occurs as the two states come close in energy. To fix this problem, a phase factor that forces a sign change in the effective SOC at the crossing point x_s can be added, leading to an excellent agreement with the exact result.[13] However, this simple fix is limited to model systems, since it requires a priori knowledge of x_s. Moreover, the contracted spin-diabatic approach to TSH is difficult to generalize for a larger number of electronic states.[13] In contrast, such problems do not exist in the GAIMS method, and its results for this one-dimensional system highlight the accuracy of the IFG and the saddle-point approximations. Importantly, this model system also validates the naive spawning criterion (Eq.(8)) used to spawn TBFs in a state with different spin multiplicity. All the runs leading to the results presented in Fig. 2 indeed underwent only one spawning event. This behavior contrasts with that of the spin-diabatic TSH dynamics, where a large number of *hops* between states are observed.[13] As discussed in detail in the AIMS literature,[22, 35] improving the spawning criterion would surely result in an even better match with the exact result. We intend to investigate potential improvements in the spawning criteria for ISC in future research.

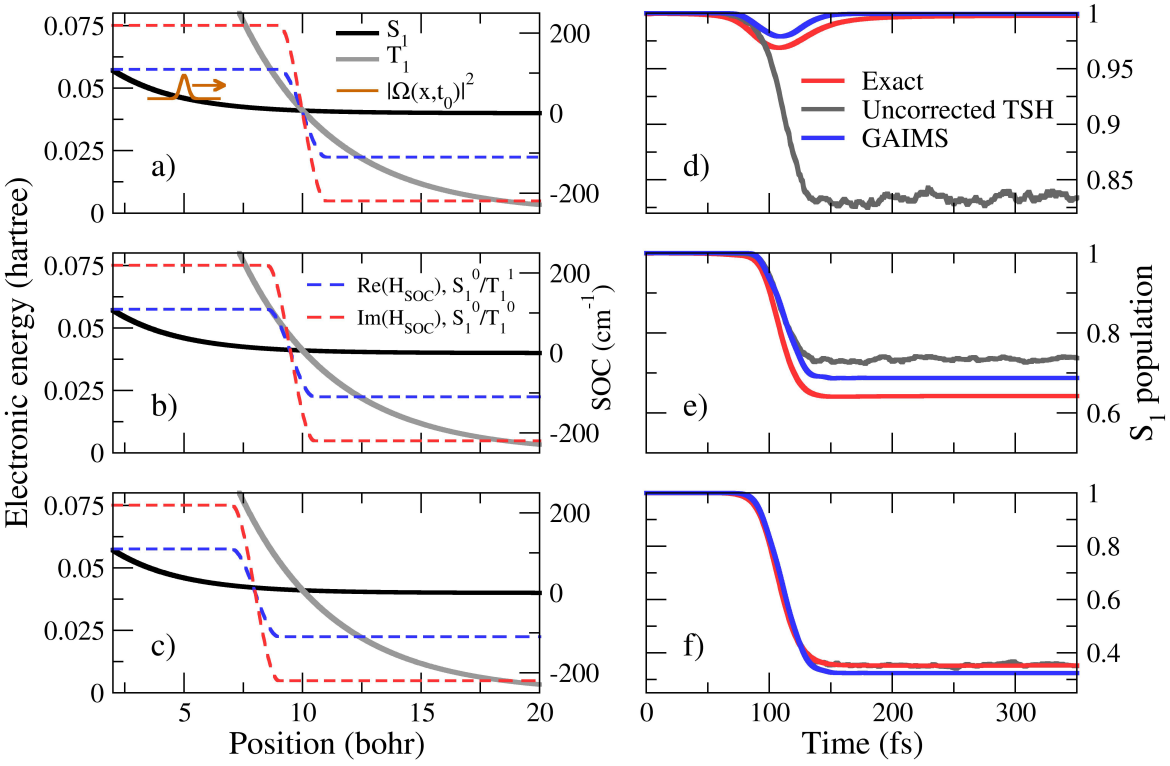

Figure 2. GAIMS applied to a one-dimensional model system with one singlet and one triplet state. a-c): Description of the model system – potential energy curves (black and gray lines), SOC matrix elements (dashed lines), for the case a) x_s=10 bohr, b) x_s=9.5 bohr, and c) x_s=8 bohr. d-f): Population in the singlet state for the three corresponding x_s values. GAIMS (blue) is compared with an exact solution of the time-dependent Schrödinger equation (red) and TSH in a spin-diabatic representation with no phase factor (gray), taken from Ref. [13].

Having shown that GAIMS provides an accurate description of ISCs for different SOC strengths, we now move to an example of its real *raison d'être*, namely the study of ISC processes in molecular systems. We choose for this purpose the nonadiabatic dynamics of thioformaldehyde, H_2CS, in its first singlet excited state. The first excited electronic state (S_1) of H_2CS has $n\pi^*$ character in the Franck-Condon region and its 0-0 transition energy has been experimentally determined at 2.033 eV.[39] Two triplet states lie close to S_1: $T_1(n\pi^*)$ and $T_2(\pi\pi^*)$. When the excited-state dynamics of H_2CS is initiated in S_1, we therefore expect to observe a direct application of the El-Sayed rules[40] – $S_1(n\pi^*)$ should be more strongly coupled to $T_2(\pi\pi^*)$ *via* SOC than to $T_1(n\pi^*)$ as a result of the change in orbital type. We performed GAIMS dynamics considering the first four electronic states of H_2CS (S_0, S_1, T_1, and T_2), using SA(4)-CASSCF(4/3)/6-31G* in Molpro[41] for 20 Wigner-sampled initial conditions. This level of theory places S_1 at 2.26 eV above the ground state in the Franck-Condon region. We present here the first 200 fs of dynamics in S_1 and will mostly comment on the GAIMS algorithm. This application is intended to provide a molecular test system for GAIMS dynamics and does not seek to obtain a complete and quantitatively accurate physical picture of the nonradiative relaxation of H_2CS (which might require larger basis sets and dynamic electron correlation).

The small yet sizable population of T_2 shortly after the beginning of the excited-state dynamics confirms the El-Sayed rule (Fig. 3), while T_1 appears to be only weakly populated in the same time window. This immediate, yet weak, population of triplet states upon photoexcitation in S_1 has also been observed for the parent molecule acetone,[42] although the population transfer is even weaker in this latter case. The total number of TBFs in the different electronic states grows quickly during the dynamics (orange line in Fig. 3), reaching a total value of 326 TBFs, among which 306 evolve in triplet states. From an initial TBF evolving in S_1, GAIMS rapidly starts to spawn TBFs in both T_2 and T_1, even though a sizable amount of population is eventually only transferred to T_2. To further analyze the dynamics, we present in Fig. 3 (upper panel) a depiction of the C=S bond length and electronic population for each of the TBFs. This representation highlights the growing number of TBFs in T_1 (red) and T_2 (blue) over the course of the simulation and depicts the different dynamics they experience, evolving in electronic states of differing electronic character. Hence, the dynamics of TBFs in T_1 is closer to those in S_1 – both exhibiting an $n\pi^*$ character – while the $\pi\pi^*$ character of TBFs evolving in T_2 is consistent with the longer average C=S bond length. As noted before, population transfer between singlet and triplet TBFs due to SOC is limited in the timescale of this simulation and the projection is mostly dominated by the TBFs evolving in S_1.

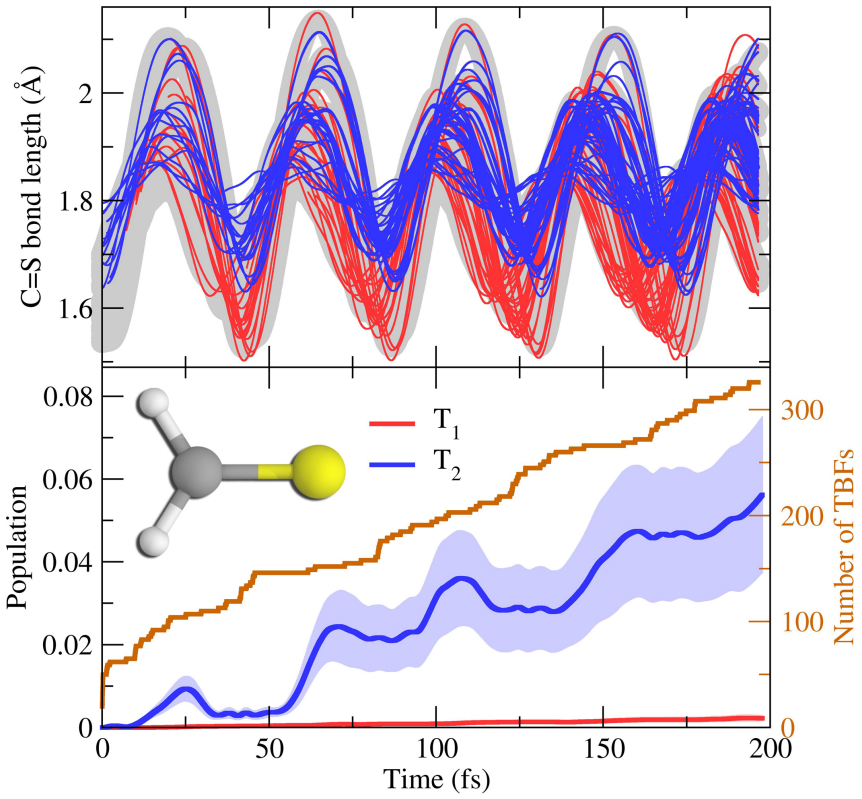

Figure 3. GAIMS dynamics of thioformaldehyde after photoexcitation to S_1. Upper panel: C=S bond length for all TBFs produced during GAIMS dynamics. The width of each line is proportional to the population carried by the TBF. TBFs are associated with the S_1 (light gray), T_1 (red), or T_2 (blue) electronic state. Lower panel: population of the two triplet states during GAIMS dynamics, averaged over 20 initial conditions (light area indicates the standard error). The total number of TBFs is given in orange.

IV. Conclusion

In this Communication, we presented a generalization of the Full and Ab Initio Multiple Spawning methods to the description of internal conversion and intersystem crossing processes, both treated on an equal footing. The derivation of GFMS and GAIMS uses a spin-diabatic formalism and the implementation of GAIMS has been validated both with a model system and with a molecular application, the nonadiabatic dynamics of thioformaldehyde. This work will be followed by an extensive study of the interplay between the TBFs and the development of improved rules for ISC-triggered spawning that will minimize the number of unpopulated TBFs on triplet states. GAIMS opens the door for complete simulation of deactivation pathways in molecules and, when combined with GPU-accelerated electronic structure codes[43-46], will be used to study the competition between internal conversion and intersystem crossing in both organic molecules and organometallic complexes.

V. Acknowledgments

This work was supported by the AMOS program within the Chemical Sciences, Geosciences and Biosciences Division of the Office of Basic Energy Sciences, Office of Science, US Department of Energy. The authors thank G. Granucci and M. Persico for sharing the numerical results reported in Ref. [13]. BFEC acknowledges the Swiss National Science Foundation for the fellowship P2ELP2_151927 and CR thanks the uni:docs program of the University of Vienna for financing his PhD and travel to Stanford.

References

1. Marian, C. M., Spin-orbit coupling and intersystem crossing in molecules. *WIREs Comput. Mol. Sci.* **2012,** *2* (187-20).
2. Parker, D. S. N.; Minns, R. S.; Penfold, T. J.; Worth, G. A.; Fielding, H. H., Ultrafast dynamics of the S-1 excited state of benzene. *Chem. Phys. Lett.* **2009,** *469* (1-3), 43-47.
3. Richter, M.; Marquetand, P.; González-Vázquez, J.; Sola, I.; González, L., Femtosecond Intersystem Crossing in the DNA Nucleobase Cytosine. *J. Phys. Chem. Lett.* **2012,** *3* (21), 3090--3095.
4. Martínez-Fernández, L.; Corral, I.; Granucci, G.; Persico, M., Competing ultrafast intersystem crossing and internal conversion: a time resolved picture for the deactivation of 6-thioguanine. *Chem. Sci.* **2014,** *5*, 1336.
5. Chergui, M., On the interplay between charge, spin and structural dynamics in transition metal complexes. *Dalton T* **2012,** *41* (42), 13022-13029.
6. Yersin, H.; Rausch, A. F.; Czerwieniec, R.; Hofbeck, T.; Fischer, T., The triplet state of organo-transition metal compounds. Triplet harvesting and singlet harvesting for efficient OLEDs. *Coord. Chem. Rev.* **2011,** *255* (21), 2622--2652.
7. Kinoshita, T.; Dy, J. T.; Uchida, S.; Kubo, T.; Segawa, H., Wideband dye-sensitized solar cells employing a phosphine-coordinated ruthenium sensitizer. *Nat. Photonics* **2013,** *7* (7), 535-539.
8. Heitz, M. C.; Ribbing, C.; Daniel, C., Spin-orbit induced radiationless transitions in organometallics: Quantum simulation of the intersystem crossing processes in the photodissociation of HCo(CO)(4). *J. Chem. Phys.* **1997,** *106* (4), 1421-1428.
9. Persico, M.; Granucci, G., An overview of nonadiabatic dynamics simulations methods, with focus on the direct approach versus the fitting of potential energy surfaces. *Theor. Chem. Acc.* **2014,** *133*, 1526.
10. Minns, R. S.; Parker, D. S. N.; Penfold, T. J.; Worth, G. A.; Fielding, H. H., Competing ultrafast intersystem crossing and internal conversion in the "channel 3" region of benzene. *Phys. Chem. Chem. Phys.* **2010,** *12* (48), 15607-15615.
11. Richter, M.; Marquetand, P.; González-Vázquez, J.; Sola, I.; González, L., SHARC: ab Initio Molecular Dynamics with Surface Hopping in the Adiabatic Representation Including Arbitrary Couplings. *J. Chem. Theory Comput.* **2011,** *7*, 1253-1258.
12. Fu, B. N.; Shepler, B. C.; Bowman, J. M., Three-State Trajectory Surface Hopping Studies of the Photodissociation Dynamics of Formaldehyde on ab Initio Potential Energy Surfaces. *J. Am. Chem. Soc.* **2011,** *133* (20), 7957-7968.
13. Granucci, G.; Persico, M.; Spighi, G., Surface hopping trajectory simulations with spin-orbit and dynamical couplings. *J. Chem. Phys.* **2012,** *137* (22), 22A501.
14. Cui, G. L.; Thiel, W., Generalized trajectory surface-hopping method for internal conversion and intersystem crossing. *J. Chem. Phys.* **2014,** *141* (12).
15. de Carvalho, F. F.; Tavernelli, I., Nonadiabatic dynamics with intersystem crossings: A time-dependent density functional theory implementation. *J. Chem. Phys.* **2015,** *143* (22).
16. Mai, S.; Marquetand, P.; Gonzalez, L., A General Method to Describe Intersystem Crossing Dynamics in Trajectory Surface Hopping. *Int. J. Quantum Chem.* **2015,** *115* (18), 1215-1231.
17. Rajak, K.; Maiti, B., Trajectory surface hopping study of the O(P-3) + C2H2 reaction dynamics: Effect of collision energy on the extent of intersystem crossing. *J. Chem. Phys.* **2014,** *140* (4), 044314.
18. Granucci, G.; Persico, M., Critical appraisal of the fewest switches algorithm for surface hopping. *J. Chem. Phys.* **2007,** *126*, 134114.
19. Tully, J. C., Molecular dynamics with electronic transitions. *J. Chem. Phys.* **1990,** *93*, 1061-1071.
20. Ben-Nun, M.; Martínez, T. J., Nonadiabatic molecular dynamics: Validation of the multiple spawning method for a multidimensional problem. *J. Chem. Phys.* **1998,** *108* (17), 7244-7257.

21. Martínez, T. J.; Ben-Nun, M.; Levine, R. D., Multi-electronic-state molecular dynamics: A wave function approach with applications. *J. Phys. Chem.* **1996,** *100* (19), 7884-7895.
22. Ben-Nun, M.; Martínez, T. J., Ab Initio Quantum Molecular Dynamics. *Adv. Chem. Phys.* **2002,** *121*, 439-512.
23. Ben-Nun, M.; Quenneville, J.; Martínez, T. J., Ab initio multiple spawning: Photochemistry from first principles quantum molecular dynamics. *J. Phys. Chem. A* **2000,** *104* (22), 5161-5175.
24. Yang, S.; Martínez, T. J., Ab Initio Multiple Spawning: First Principles Dynamics Around Conical Intersections. In *Conical Intersections: Theory, Computation and Experiment*, Domcke, W.; Yarkony, D. R.; Köppel, H., Eds. World Scientific Publishing Co. Pte. Ltd.: 2011; Vol. 17, pp 347-374.
25. Almlöf, J.; Gropen, O., Relativistic Effects in Chemistry. In *Reviews in Computational Chemistry*, Lipkowitz, K. B.; Boyd, D. B., Eds. VCH Publishers: New York, 1996; Vol. 8, p 203.
26. The additional terms in the Breit-Pauli Hamiltonian are not considered here.
27. Fedorov, D. G.; Koseki, S.; Schmidt, M. W.; Gordon, M. S., Spin-orbit coupling in molecules: chemistry beyond the adiabatic approximation. *Int. Rev. Phys. Chem.* **2003,** *22* (3), 551-592.
28. Dolg, M.; Cao, X. Y., Relativistic Pseudopotentials: Their Development and Scope of Applications. *Chem. Rev.* **2012,** *112* (1), 403-480.
29. Yarkony, D. R., Spin-Forbidden Chemistry within the Breit-Pauli Approximation. *Int. Rev. Phys. Chem.* **1992,** *11* (2), 195-242.
30. Reiher, M.; Wolf, A., *Relativistic Quantum Chemistry: the Fundamental Theory of Molecular Science*. WILEY-VCH Verlag GmbH & Co. KGaA,: Weinheim, 2009.
31. Dyall, K. G.; Knut Fægri, J., *Introduction to Relativistic Quantum Chemistry*. Oxford University Press, Inc.: New York, 2007.
32. Born, M.; Huang, K., *Dynamical Theory of Crystal Lattices*. Clarendon, Oxford: 1954.
33. Worth, G. A.; Robb, M. A.; Lasorne, B., Solving the time-dependent Schrödinger equation for nuclear motion in one step: direct dynamics of non-adiabatic systems. *Mol. Phys.* **2008,** *106* (16-18), 2077--2091.
34. Shalashilin, D. V., Quantum mechanics with the basis set guided by Ehrenfest trajectories: Theory and application to spin-boson model. *J. Chem. Phys.* **2009,** *130*, 244101.
35. Yang, S.; Coe, J. D.; Kaduk, B.; Martínez, T. J., An "optimal" spawning algorithm for adaptive basis set expansion in nonadiabatic dynamics. *J. Chem. Phys.* **2009,** *130* (13).
36. In the absence of an external magnetic field, the sublevels of a given electronic state with S>0 are exactly degenerate. Therefore, the TBFs for different sublevels resulting from a given spawning event will follow the very same classical trajectory, implying that the corresponding complex coefficients can be evolved on the support of only one trajectory as shown in Figure 2. This observation leads to substantial computational savings for the propagation of the Gaussian functions. There is no approximation involved since all sublevel coefficients are still explicitly considered and time-evolved.
37. Sulc, M.; Hernandez, H.; Martínez, T. J.; Vanicek, J., Relation of exact Gaussian basis methods to the dephasing representation: Theory and application to time-resolved electronic spectra. *J. Chem. Phys.* **2013,** *139* (3).
38. Martínez, T. J.; Levine, R. D., Non-adiabatic molecular dynamics: Split-operator multiple spawning with applications to photodissociation. *J. Chem. Soc., Faraday Trans.* **1997,** *93* (5), 941-947.
39. Clouthier, D. J.; Ramsay, D. A., The Spectroscopy of Formaldehyde and Thioformaldehyde. *Annu. Rev. Phys. Chem.* **1983,** *34*, 31-58.
40. Elsayed, M. A., Triplet State - Its Radiative and Nonradiative Properties. *Acc. Chem. Res.* **1968,** *1* (1), 8.
41. Werner, H. J.; Knowles, P. J.; Knizia, G.; Manby, F. R.; Schutz, M., Molpro: a general-purpose quantum chemistry program package. *WIREs Comput. Mol. Sci.* **2012,** *2* (2), 242-253.

42. Favero, L.; Granucci, G.; Persico, M., Dynamics of acetone photodissociation: a surface hopping study. *Phys. Chem. Chem. Phys.* **2013,** *15* (47), 20651--20661.
43. Hohenstein, E. G.; Luehr, N.; Ufimtsev, I. S.; Martínez, T. J., An atomic orbital-based formulation of the complete active space self-consistent field method on graphical processing units. *J. Chem. Phys.* **2015,** *142* (22).
44. Snyder, J. W.; Hohenstein, E. G.; Luehr, N.; Martínez, T. J., An atomic orbital-based formulation of analytical gradients and nonadiabatic coupling vector elements for the state-averaged complete active space self-consistent field method on graphical processing units. *J. Chem. Phys.* **2015,** *143* (15).
45. Hohenstein, E. G.; Bouduban, M. E. F.; Song, C. C.; Luehr, N.; Ufimtsev, I. S.; Martínez, T. J., Analytic first derivatives of floating occupation molecular orbital-complete active space configuration interaction on graphical processing units. *J. Chem. Phys.* **2015,** *143* (1).
46. Fales, B. S.; Levine, B. G., Nanoscale Multireference Quantum Chemistry: Full Configuration Interaction on Graphical Processing Units. *J. Chem. Theory Comput.* **2015,** *11* (10), 4708-4716.